

Heterologous expression of a cryptic gene cluster from *Marinomonas fungiae* affords a novel tricyclic peptide marinomonasin

メタデータ	言語: eng 出版者: 公開日: 2022-01-27 キーワード (Ja): キーワード (En): 作成者: Kaweewan, Issara, Nakagawa, Hiroyuki, Kodani, Shinya メールアドレス: 所属:
URL	<a href="http://hdl.handle.net/10297/00028565">http://hdl.handle.net/10297/00028565</a>

1 Title: Heterologous expression of a cryptic gene cluster from *Marinomonas fungiae*  
2 affords a novel tricyclic peptide marinomonasin  
3 Running headline: novel tricyclic peptide marinomonasin  
4 Authors: Issara Kaweewan<sup>1</sup>, Hiroyuki Nakagawa<sup>2,3</sup>, and Shinya Kodani<sup>1,4,5\*</sup>  
5 Affiliations: <sup>1</sup>Faculty of Agriculture, Shizuoka University, Shizuoka, Japan; <sup>2</sup>Food  
6 Research Institute, National Agriculture and Food Research Organization (NARO),  
7 Ibaraki, Japan; <sup>3</sup>Advanced Analysis Center, National Agriculture and Food Research  
8 Organization (NARO), Ibaraki, Japan; <sup>4</sup>Shizuoka Institute for the Study of Marine  
9 Biology and Chemistry, Shizuoka University, Shizuoka, Japan; <sup>5</sup>College of Agriculture,  
10 Academic Institute, Shizuoka University, Shizuoka, Japan  
11 \*To whom correspondence should be addressed: Shinya Kodani, College of  
12 Agriculture, Academic Institute, Shizuoka University, 836 Ohya, Suruga-ku, Shizuoka  
13 422-8529 Japan, Tel/Fax; +81(54)238-5008, E-mail; kodani.shinya@shizuoka.ac.jp,  
14 ORCID:0000-0002-6792-1184

15

16 **Abstract**

17 The  $\omega$ -ester-containing peptides are a group of ribosomally synthesized and  
18 posttranslationally modified peptides. The biosynthetic gene clusters of  $\omega$ -ester-  
19 containing peptides commonly include ATP-grasp ligase coding genes and are  
20 distributed over the genomes of a wide variety of bacteria. A new biosynthetic gene  
21 cluster of  $\omega$ -ester-containing peptides was found in the genome sequence of the marine  
22 proteobacterium *Marinomonas fungiae*. Heterologous production of a new tricyclic  
23 peptide named marinomonasin was accomplished using the biosynthetic gene cluster in  
24 *Escherichia coli* expression host strain BL21 (DE3). By ESI-MS and NMR  
25 experiments, the structure of marinomonasin was determined to be a tricyclic peptide 18  
26 amino acids in length with one ester and two isopeptide bonds in the molecule. The  
27 bridging patterns of the three intramolecular bonds were determined by the  
28 interpretation of HMBC and NOESY data. The bridging pattern of marinomonasin was  
29 unprecedented in the  $\omega$ -ester-containing peptide group. The results indicated that the  
30 ATP-grasp ligase for the production of marinomonasin was a novel enzyme possessing  
31 bifunctional activity to form one ester and two isopeptide bonds.

32

33 **Keywords:** heterologous expression; ATP-grasp ligase; biosynthesis;  $\omega$ -ester-

34 containing peptide

35

36 Key points

37 New tricyclic peptide marinomonasin was heterologously produced in *Escherichia coli*.

38 Marinomonasin contained one ester and two isopeptide bonds in the molecule.

39 The bridging pattern of intramolecular bonds was novel.

40

41

## 42 **Introduction**

43 Ribosomally synthesized and posttranslationally modified peptides (RiPPs) include  
44 more than twenty subclasses (Budisa 2013). By genome mining, the biosynthetic gene  
45 clusters (BGCs) of a new class of RiPPs,  $\omega$ -ester-containing peptides (OEPs), were  
46 found to be distributed over the genomes of bacteria (Lee et al. 2020b). This class of  
47 RiPPs was renamed graspeptides because the biosynthetic system included ATP-grasp  
48 ligase (Montalban-Lopez et al. 2021). The minimum set of BGCs of OEPs  
49 (graspeptides) was indicated to consist of two genes (precursor and ATP-grasp ligase  
50 coding genes) that are essential for the production of mature cyclic peptides. BGCs with  
51 at least two essential genes were found by searching the genome data of bacteria in the  
52 database. A total of ~1500 candidate OEPs (graspeptides) were indicated based on the  
53 similarity of the amino acid sequences of precursor peptides, and the OEPs  
54 (graspeptides) were classified into 12 groups (Lee et al. 2020b).

55 Among the 12 groups, group 1 contained cyanobacterial peptides called microviridins  
56 (Dehm et al. 2019; Fujii et al. 2000; Ishitsuka et al. 1990; Murakami et al. 1997; Okino  
57 et al. 1995; Reshef and Carmeli 2006; Rohrlack et al. 2003; Shin et al. 1996). The  
58 structure of microviridins commonly contains two ester and one isopeptide bond  
59 biosynthesized by two ATP-grasp ligases (Philmus et al. 2008; Ziemert et al. 2008).

60 Attempts have been reported to generate new cyclic peptides by genetic engineering  
61 utilizing the intramolecular macrocyclization mechanism of the core peptide in  
62 microviridins (Ahmed et al. 2017; Gatte-Picchi et al. 2014; Reyna-Gonzalez et al. 2016;  
63 Weiz et al. 2011; Weiz et al. 2014; Zhang et al. 2018; Ziemert et al. 2010). In the  
64 genomes of bacteria belonging to Proteobacteria, Bacteroidetes, and Cyanobacteria,  
65 BGCs of microviridin-type peptides were found to be widely distributed (Ahmed et al.  
66 2017). Utilizing the BGC of the marine proteobacterium *Grimontia marina*,  
67 heterologous production of a new microviridin-type peptide named grimoviridin was  
68 reported (Unno et al. 2020). Recently, chryseoviridin, a new type of multicore RiPP,  
69 was produced by *in vitro* synthesis using the precursor peptide CdnA3 and the ATP-  
70 grasp ligase CdnC of *Chryseobacterium gregarium* (Zhao et al. 2021). Interestingly, the  
71 ATP-grasp ligase CdnC was found to install single and bicyclic  $\omega$ -ester rings on  
72 multiple domains of the precursor peptide CdnA3 (Zhao et al. 2021). Regarding the  
73 peptides in group 2, heterologous production of the peptide plesiocin was reported using  
74 the BGC of the marine myxobacterium *Plesiocystis pacifica* (Lee et al. 2020a; Lee et al.  
75 2017). Plesiocin contained four repeats of a distinct hairpin-like bicyclic structure  
76 containing two ester bonds each and showed potent inhibitory activity against proteases.  
77 A peptide named thuringinin (group 3) was produced using BGC derived from *Bacillus*

78 *thuringiensis serovar huazhongensis* in the same manner as plesiocin (Roh et al. 2019).  
79 Similar to plesiocin, thuringinin had three tandemly repeating hairpin-like structures  
80 with two ester bonds each. The bridging pattern of ester bonds was different from that  
81 of plesiocin. In addition, new OEPs (OEP4-1, OEP5-1, OEP6-1) were produced using  
82 the BGCs of groups 4, 5, and 6, respectively (Lee et al. 2020b). Recently, we reported  
83 the heterologous production of a new peptide named prunipeptin belonging to group 11  
84 (Unno and Kodani 2021). Prunipeptin was determined to be a bicyclic peptide  
85 possessing one ester and one isopeptide bond. Interestingly, OEPs (graspeptides) had  
86 diverse intramolecular bond formation patterns in the seven groups (groups 1-6 and 11).  
87 These data indicated that the specificity of the ATP-grasp enzyme of each group  
88 determines the bridge formation pattern of intramolecular bonds. Further investigation  
89 on OEPs (graspeptides) in the rest of the groups is needed to clarify the characteristics  
90 of the ATP-grasp enzyme and generate new cyclic peptides.

91 Based on this background, we accomplished the heterologous production of a new  
92 tricyclic peptide named marinomonasin using BGC of the marine proteobacterium  
93 *Marinomonas fungiae*. By analyses of MS and NMR data, the structure of  
94 marinomonasin was determined. Here, we describe the heterologous production,  
95 isolation and structure determination of marinomonasin.

96 **Materials and methods**

97 **Bacterial strain**

98 *Marinomonas fungiae* strain JCM 18476<sup>T</sup> was obtained from Japan Collection of  
99 Microorganisms (JCM), RIKEN BioResource Research Center, Ibaraki, Japan.

100 **Construction of the expression vector pET41a-18476ABCD**

101 Genomic DNA was extracted from *M. fungiae* strain JCM 18476<sup>T</sup> using DNeasy Blood  
102 & Tissue Kit (Qiagen, Venlo, Netherlands). The diluted DNA was used as a template  
103 for PCR amplification. The gene fragment of marinomonasin containing four genes in  
104 Fig. 1A (2179 bp) was amplified by PCR with a primer pair (18476-ATP-F-XbaI and  
105 18476-ATP-R-KpnI, Table S1 and Figure S1) using EmeraldAmp PCR Master Mix  
106 (Takara Bio Inc., Shiga, Japan), following the manufacturer's instructions. Amplified  
107 PCR product was purified using NucleoSpin Gel and PCR Clean-up (Macherey-Nagel,  
108 Germany). The insert DNA fragment and the pET-41a(+) vector were double-digested  
109 with *Xba*I and *Kpn*I-HF (New England Biolabs, Ipswich, MA, USA), following the  
110 manufacturer's instructions. To obtain the vector pET41a-18476ABCD, the digested  
111 insert DNA fragment and the digested vector pET-41a (+) were ligated using Ligation-  
112 Convenience Kit (Nippon Gene Co., Ltd., Tokyo, Japan), according to manufacturer's

113 instructions. The 5  $\mu$ L of ligation mixture was transformed into *Escherichia coli* DH5 $\alpha$   
114 cells, and the transformants were spread on LB agar plates containing kanamycin (30  
115  $\mu$ g/mL, final concentration). The vector pET41a-18476ABCD was extracted and  
116 purified using FastGene Plasmid Mini Kit (Nippon Genetics Co., Ltd., Tokyo, Japan),  
117 following the manufacturer's instructions. For heterologous expression of  
118 marinomonasin, the vector pET41a-18476ABCD was transformed into the expression  
119 host *E. coli* BL21(DE3) by chemical competence method.

#### 120 **Construction of the expression vector pET41a-18476ABC**

121 To construct the expression vector pET41a-18476ABC containing *marA*, *marB* and the  
122 uncharacterized protein coding gene (accession number: CUB04734.1), the vector  
123 pET41a-18476ABCD was used as a DNA template for PCR amplification with a primer  
124 pair (18476-ATP-Del-KpnI-F and 18476-ATP-Del-ABC-KpnI-R, in Table S1 and  
125 Figure S2), using EmeraldAmp PCR Master Mix (Takara Bio Inc., Shiga, Japan),  
126 following the manufacturer's instructions. Amplified PCR product was purified using  
127 NucleoSpin Gel and PCR Clean-up (Macherey-Nagel, Germany) and was digested with  
128 *KpnI*-HF (New England Biolabs, Ipswich, MA, USA), following the manufacturer's  
129 instructions. To obtain the vector pET41a-18476ABC, self-ligation was performed  
130 using Ligation-Convenience Kit (Nippon Gene Co., Ltd., Tokyo, Japan), according to

131 manufacturer's instructions. The 5  $\mu$ L of ligation mixture was transformed into *E. coli*  
132 DH5 $\alpha$  cells, and the transformants were spread on LB agar plates containing kanamycin  
133 (30  $\mu$ g/mL, final concentration). The vector pET41a-18476ABC was extracted and  
134 purified using FastGene Plasmid Mini Kit (Nippon Genetics Co., Ltd., Tokyo, Japan),  
135 following the manufacturer's instructions. Finally, the vector pET41a-18476ABC was  
136 transformed into the expression host *E. coli* BL21(DE3) by chemical competence  
137 method.

#### 138 **Construction of the expression vector pET41a-18476AB**

139 To construct the expression vector pET41a-18476AB containing *marA* and *marB*, the  
140 vector pET41a-18476ABCD was used as a DNA template for PCR amplification with  
141 the primer pair (18476-ATP-Del-KpnI-F and 18476-ATP-Del-AB-KpnI-R, in Table S1  
142 and Figure S3), using EmeraldAmp PCR Master Mix (Takara Bio Inc., Shiga, Japan),  
143 following the manufacturer's instructions. Amplified PCR product was purified using  
144 NucleoSpin Gel and PCR Clean-up (Macherey-Nagel, Germany) and was digested with  
145 *KpnI*-HF (New England Biolabs, Ipswich, MA, USA), following the manufacturer's  
146 instructions. To obtain the vector pET41a-18476AB, self-ligation was performed using  
147 Ligation-Convenience Kit (Nippon Gene Co., Ltd., Tokyo, Japan), according to  
148 manufacturer's instructions. The 5  $\mu$ L of ligation mixture was transformed into *E. coli*

149 DH5 $\alpha$  cells, and the transformants were spread on LB agar plates containing kanamycin  
150 (30  $\mu\text{g}/\text{mL}$ , final concentration). The vector pET41a-18476AB was extracted and  
151 purified using FastGene Plasmid Mini Kit (Nippon Genetics Co., Ltd., Tokyo, Japan),  
152 following the manufacturer's instructions. Finally, the vector pET41a-18476AB was  
153 transformed into the expression host *E. coli* BL21(DE3) by chemical competence  
154 method.

#### 155 **Heterologous expression of marinomonasin**

156 *E. coli* BL21(DE3) harboring the vector pET41a-18476ABCD, pET41a-18476ABC or  
157 pET41a-18476AB was cultured using modified basal agar medium (MBM) containing  
158 kanamycin (30  $\mu\text{g}/\text{mL}$ , final concentration) and isopropyl- $\beta$ -D-thiogalactopyranoside  
159 (IPTG) (0.1 mM, final concentration) at 30 $^{\circ}\text{C}$  for 24 h. The modified basal agar medium  
160 was prepared by adding inorganic compounds ( $\text{K}_2\text{SO}_4$ , 2 g;  $\text{K}_2\text{HPO}_4$ , 3 g; NaCl, 1 g;  
161  $\text{NH}_4\text{Cl}$ , 5 g;  $\text{MgSO}_4 \cdot 7\text{H}_2\text{O}$ , 80 mg;  $\text{CuCl}_2$ , 0.5 mg;  $\text{MnSO}_4 \cdot \text{H}_2\text{O}$ , 0.35 mg;  $\text{FeCl}_3$ , 0.5  
162 mg;  $\text{CaCl}_2 \cdot 2\text{H}_2\text{O}$ , 0.5 mg) and 15 g agar in 1 L of distilled water, followed by adjusting  
163 pH to 7.3. After autoclaving, the medium was supplemented with separately sterilized  
164 glucose and yeast extracts at final concentrations of 0.25 and 0.4%, respectively.  
165 Bacterial cells on agar medium surface were harvested using laboratory spatula and  
166 were extracted with double volume of MeOH. After centrifugation, the extract was

167 analyzed by high-performance liquid chromatography (HPLC) using Wakopak Handy  
168 ODS column (4.6 × 250 mm, Fujifilm Wako Pure Chemical Co., Japan) with gradient  
169 mode using solvent A (MeCN containing 0.05% TFA) and solvent B (H<sub>2</sub>O containing  
170 0.05% TFA). The gradient mode was performed by increasing percentage of solvent A  
171 from 5% to 25% during 20 min. The UV detector was set at 220 nm and the flow rate  
172 was set at 1 mL/min.

### 173 **Isolation of marinomonasin**

174 *E. coli* BL21(DE3) harboring the vector pET41a-18476AB was cultured using total 4 L  
175 of the modified basal agar medium (MBM) containing kanamycin (30 µg/mL, final  
176 concentration) and IPTG (0.1 mM, final concentration) at 30 °C for 24 h. Bacterial cells  
177 on agar medium surface were harvested using laboratory spatula and were extracted  
178 with double volume of MeOH. After centrifugation (4000 rpm, 10 min), the supernatant  
179 was removed from insoluble material and concentrated by rotary evaporation. In order  
180 to obtain pure compound, the concentrated extract was repeatedly subjected to HPLC  
181 purification (Figure S4 and S6). Marinomonasin was isolated by HPLC using ODS  
182 column (Wakopak Handy ODS, 4.6 × 250 mm, Fujifilm Wako Pure Chemical Co.,  
183 Japan) with isocratic mode; 18% MeCN/water containing 0.05% TFA (Retention time;  
184 14.80 min, Fig. S6b). The UV detector was set at 220 nm and the flow rate was set at 1

185 mL/min. The pure compound obtained from HPLC was lyophilized by freeze-dryer.

186 Marinomonasin (11.5 mg) was obtained as white powder after lyophilization.

### 187 **Mass spectrometry experiments**

188 The accurate mass measurement was conducted using an ESI Orbitrap mass 158

189 spectrometer (Orbitrap Velos ETD, Thermo Fisher Scientific, Waltham, MA, USA)

190 following the previous report (Unno et al. 2020).

### 191 **NMR experiments**

192 NMR sample was prepared by dissolving 7.9 mg of marinomonasin in 500  $\mu$ L of

193 DMSO-*d*<sub>6</sub>. 1D and 2D NMR spectra were obtained from Bruker Avance800

194 spectrometer with quadrature detection following the previous report (Kodani et al.

195 2018).

### 196 **Protease inhibition assay**

197 Protease inhibition assay was performed by modified method of the previous report

198 (Unno et al. 2020). Enzyme solution (trypsin, chymotrypsin and elastase) was prepared

199 by dissolving enzyme in 50 mM Tris-HCl buffer. Trypsin from Porcine Pancreas

200 (35544-94, Nacalai Tesque, Inc., Kyoto, Japan) and chymotrypsin from Bovine

201 Pancreas (09041-84, Nacalai Tesque, Inc.) were dissolved in 50 mM Tris-HCl buffer

202 (pH 7.6) to obtain 150 U/mL and 15 U/mL enzyme solutions, respectively. Elastase  
203 from Porcine Pancreas (E1250, Sigma-Aldrich, Inc., St. Louis, MO, USA) was  
204 dissolved in 50 mM Tris-HCl buffer (pH 8.6) to obtain 0.6 U/mL enzyme solution.  
205 Substrate solution for trypsin was prepared by dissolving 43.3 mg of *N* $\alpha$ -Benzoyl-DL-  
206 arginine 4-nitroanilide hydrochloride (B4875, Sigma-Aldrich, Inc.) in 1 mL of dimethyl  
207 sulfoxide (DMSO), followed by addition of 99 mL of 50 mM Tris-HCl buffer (pH 7.6).  
208 Substrate solution for chymotrypsin was prepared by dissolving *N*-Succinyl-L-  
209 phenylalanine-*p*-nitroanilide (S2628, Sigma-Aldrich, Inc.) in 50 mM Tris-HCl buffer  
210 (pH 7.6) (final concentration of 1 mg/mL). Substrate solution for elastase was prepared  
211 by dissolving *N*-Succinyl-Ala-Ala-Ala-*p*-nitroanilide (S4760, Sigma-Aldrich, Inc.) in  
212 50 mM Tris-HCl buffer (pH 8.6) (final concentration of 1 mg/mL). For enzyme  
213 inhibition assay, 100  $\mu$ L of enzyme solution and 60  $\mu$ L of 0.4 M Tris-HCl buffer (pH  
214 7.6 for trypsin and chymotrypsin, pH 8.6 for elastase) were prepared in  
215 spectrophotometer cuvettes. The 40  $\mu$ L of marinomonasin (100  $\mu$ g/mL) was added into  
216 the mixture and the reaction mixture was pre-incubated at 37 °C for 5 min. After  
217 addition of 200  $\mu$ L of substrate solution, the absorbance at 405 nm was immediately  
218 measured ( $A_{405}$  start). The reaction mixture was incubated at 37 °C for 30 min and then  
219 the absorbance at 405 nm was measured ( $A_{405}$  end) to clarify enzyme inhibitory activity

220 of marinomanasin.

221

## 222 **Results**

### 223 **Assignment of the biosynthetic gene cluster**

224 In group 7 OEPs (graspeptides), 113 BGCs were found to be distributed mostly  
225 among Proteobacteria (Lee et al. 2020b). The BGCs of group 7 commonly contain a  
226 minimum of two genes, a precursor peptide coding gene and an ATP-grasp ligase  
227 coding gene. We found typical BGCs in the genome of the marine proteobacterium  
228 *Marinomonas fungiae*. The BGC contained two genes coding for a precursor peptide  
229 (*marA*, accession number: CUB04731.1) and an ATP-grasp ligase (*marB*, accession  
230 number: CUB04732.1), as shown in Fig. 1A. Two other genes, including an  
231 uncharacterized protein-coding gene (accession number: CUB04734.1) and a quinol  
232 monooxygenase-coding gene (accession number: CUB04736.1), existed close to the  
233 BGC (Fig. 1A), although it was unclear whether the additional two genes were involved  
234 in the biosynthesis of the OEP (graspeptide). To find analogous peptide-coding genes, a  
235 similarity search was performed by BLASTP search using the amino acid sequence of  
236 the precursor peptide gene (*marA*). Many analogous genes were found in the genomes  
237 of Proteobacteria, such as *Vibrio*, and the alignment of the genes is shown in Fig. 1B.  
238 Apparently, the leader peptide region at the *N*-terminus does not have similarity except  
239 for the short sequences H-(V/I/L)-L and G-X-W shown by bold letters in Figure 1B. On

240 the other hand, the core sequence at the C-terminus has a conserved sequence: (T/S)-K-  
241 K-X-D-X-E-T-G-E-D-X-K-G-(E/Q). We checked the production of the expected OEP  
242 (graspeptide) in *M. fungiae*. Briefly, *M. fungiae* was cultured using marine agar 2216  
243 medium. The cells of *M. fungiae* were extracted by MeOH, and the extract was analysed  
244 by HPLC and ESI-MS (data not shown). As a result, the expected peptide was not  
245 detected in the MeOH extract. Thus, we planned to perform heterologous expression of  
246 the BGC of *M. fungiae* to obtain a new OEP (graspeptide).

#### 247 **Heterologous production of marinomonasin**

248 First, we performed molecular cloning of the region including the four genes shown  
249 in Fig. 1A, considering the possibility that the two additional genes, an uncharacterized  
250 protein coding gene (CUB04734.1) and a quinol monooxygenase coding gene  
251 (CUB04736.1), might also participate in the biosynthesis. To obtain crude genomic  
252 DNA as a template for PCR, *Marinomonas fungiae* JCM18476 cells were extracted  
253 using a DNA extraction kit. The gene fragment including the four genes was amplified  
254 by PCR using template genomic DNA and primers (Table S1). The amplified DNA  
255 fragment was cut by restriction enzymes followed by ligation with the cut plasmid of  
256 pET41a (+) to give the expression vector pET41a-18476ABCD (Figure S1). The  
257 bacterium *E. coli* BL21(DE3) possessing the vector pET41a-18476ABCD was cultured

258 on modified basal agar medium containing kanamycin and isopropyl- $\beta$ -D-  
259 thiogalactopyranoside (IPTG) at 30 °C for 24 h. The cells were harvested with a  
260 laboratory spatula and extracted with a double volume of MeOH. The MeOH extract  
261 was analysed by HPLC and ESI-MS. The resulting transformant produced several  
262 peptides, including marinomonasin. To determine the essential gene set for the  
263 production of marinomonasin, two expression vectors (pET41a-18476ABC containing  
264 *marA*, *marB*, and the uncharacterized protein coding gene CUB04734.1 in Figure S2,  
265 pET41a-18476AB containing *marA* and *marB* in Figure S3) were constructed. To  
266 construct the two expression vectors (pET41a-18476ABC and pET41a-18476AB), PCR  
267 was applied using pET41a-18476ABCD as template DNA to obtain two DNA  
268 fragments (Figure S2 and S3). After the treatment of each DNA fragment with the  
269 restriction enzyme *KpnI*, ligation was performed to obtain pET41a-18476ABC or  
270 pET41a-18476AB (Figure S2 and S3), followed by transformation into *Escherichia coli*  
271 DH5 $\alpha$ . After cloning of each plasmid in *E. coli* DH5 $\alpha$ , each plasmid was transformed  
272 into *E. coli* BL21(DE3). The production of peptides was compared by HPLC among  
273 three different transformants of *E. coli* BL21(DE3) containing one of the vectors  
274 (pET41a-18476ABCD, pET41a-18476ABC, or pET41a-18476AB). The HPLC  
275 chromatographs of the MeOH extracts of all three transformants indicated exactly the

276 same profile (Figure S5). This result indicated that the essential gene set to produce  
277 marinomonasin was *marA* (precursor peptide coding gene) and *marB* (ATP-grasp ligase  
278 coding gene). The highest production yield was observed in the transformant containing  
279 pET41a-18476AB (Figure S5). Thus, the production of marinomonasin was  
280 accomplished using the transformant containing pET41a-18476AB.

### 281 **Isolation and structure determination of marinomonasin**

282 The transformant *E. coli* BL21(DE3) harbouring the vector pET41a-18476AB was  
283 cultured using modified basal agar medium. The bacterial cells were directly harvested  
284 by laboratory spatula from the agar medium and extracted with MeOH. The MeOH  
285 extract was repeatedly subjected to HPLC purification to obtain marinomonasin (Fig.  
286 S4 and S6). To determine the chemical structure, including the bridging pattern, NMR  
287 spectra ( $^1\text{H}$ ,  $^{13}\text{C}$ , DEPT-135, DQF-COSY, TOCSY, NOESY, HMBC, and HSQC) of  
288 marinomonasin dissolved in 0.5 mL of DMSO- $d_6$  were analysed (Figures S7-S39). All  
289 18 amino acids in marinomonasin were assigned using spin system identification from  
290 the 2D NMR spectral data (Figure 2 and Table S2). The peptide sequence of 18 amino  
291 acids was determined by the NOESY correlations between the  $\alpha$ -proton and amide  
292 proton of adjacent amino acids (double ended arrow in Figure 2). The bridge between  
293 Thr4 and Asp14 was determined by HMBC correlations. HMBC correlations to the  $\beta$ -

294 carbonyl carbon ( $\delta\text{C}$  171.3) from  $\beta$ -protons ( $\delta\text{H}$  2.88,  $\delta\text{H}$  3.29) of Asp14 and  $\beta$ -proton  
295 ( $\delta\text{H}$  5.34) of Thr4 were observed (Figure S39), which indicated the presence of an ester  
296 bond between the side chains of Thr4 and Asp14. The NOESY correlation between the  
297  $\epsilon$ -NH of Lys5 and the  $\gamma$ -protons of Glu13 was observed, which indicated an isopeptide  
298 bond between the side chains of Lys5 and Glu13 (Figure S31). In the same manner, the  
299 NOESY correlation between the  $\epsilon$ -NH of Lys6 and the  $\gamma$ -protons of Glu10 was observed  
300 (Figure S31), which indicated an isopeptide bond between the side chains of Lys6 and  
301 Glu10. Above all, the structure of marinomonasin was determined to be a tricyclic  
302 peptide with three intramolecular bonds, including one ester bond (Thr4/Asp14) and  
303 two isopeptide bonds (Lys5/Glu13 and Lys6/Glu10), as shown in Figure 2. To  
304 determine the molecular formula, accurate MS analysis of marinomonasin was  
305 accomplished in positive ion mode (Figure S40). Marinomonasin gave an ion peak of  
306 decarboxylated molecule  $[\text{M} - \text{COOH} + \text{Na} + \text{H}]^{2+}$   $m/z$  944.9419 (the calculated  $m/z$   
307 value was 944.9453:  $\text{C}_{78}\text{H}_{128}\text{O}_{28}\text{N}_{23}\text{SNa}$ ). In the NMR spectrum, all amino acids were  
308 assigned, and no decarboxylated residue was observed. Therefore, we concluded that  
309 decarboxylation occurred as fragmentation of the ionization process of ESI-MS.

### 310 **Protease inhibition assay**

311 As several OEPs (graspeptides), including plesiocin (Lee et al. 2020a; Lee et al.  
312 2017) and microviridins (Dehm et al. 2019; Fujii et al. 2000; Ishitsuka et al. 1990;  
313 Murakami et al. 1997; Okino et al. 1995; Reshef and Carmeli 2006; Rohrlack et al.  
314 2003; Shin et al. 1996), were reported to possess inhibitory activity against proteases,  
315 we performed protease inhibitory assays using trypsin, chymotrypsin, and elastase.  
316 Marinomonasin did not show inhibitory activity against all tested proteases at a  
317 concentration of 100 µg/mL (Table S3).  
318

319 **Discussion**

320 Several OEPs (graspeptides), including microviridins, plesiocin, and chryseoviridin,  
321 were characterized as protease inhibitors. Among the inhibitors, the inhibitory  
322 mechanism of microviridin J was clarified at the molecular level by X-ray  
323 crystallographic analysis of cocrystals of microviridin J and trypsin (Weiz et al. 2014).  
324 Microviridin J binds to the hydrophobic pocket located on the surface of trypsin by  
325 forming a substrate-like trypsin binding motif. The methyl group of the Thr4 side chain  
326 of microviridin J points towards Leu99 of the S2 pocket, while the Arg5 side chain  
327 interacts with the carboxyl group of Asp189 at the bottom of the S1 pocket (Weiz et al.  
328 2014). In this report, we tested marinomonasin against serine proteases, including  
329 trypsin, chymotrypsin, and elastase. However, no protease inhibitory activity was  
330 observed in the marinomonasin assay. The amino acid sequence and bridging pattern of  
331 marinomonasin were different from those of the inhibitory peptides (microviridins,  
332 plesiocin and chryseoviridin). Marinomonasin may not have such a strong binding  
333 affinity to active pockets of proteases as other protease inhibitory OEPs (graspeptides).

334 The topology of bridging patterns of OEPs (graspeptides) that were determined thus  
335 far is summarized in Figure 3B. In groups 1, 5, and 11, OEPs (graspeptides) possess  
336 intramolecular isopeptide bond in addition to ester bonds. In group 1, the two ATP-

337 grasp ligases (MdnB and MdnC in the case of microviridin B) were indicated to form  
338 two ester bonds and one isopeptide bond (Hemscheidt 2012; Ziemert et al. 2008). The  
339 two ligases have different functions: the ligase MdnC catalyses the formation of two  
340 ester bonds, and the other ligase MdnB catalyses the formation of isopeptide bond (Li et  
341 al. 2016). Recently, chryseoviridin, a peptide with single and bicyclic  $\omega$ -ester rings, was  
342 produced by *in vitro* synthesis using the ATP-grasp ligase CdnC of *Chryseobacterium*  
343 *gregarium* (Zhao et al. 2021). In a previous report (Lee et al. 2020b), the BGC of *C.*  
344 *gregarium* was classified into group 1 based on the similarity of the amino acid  
345 sequence of the precursor peptide. However, the ester-forming pattern of chryseoviridin  
346 was novel (Figure 3B), and it is proposed to be classified into a subclass of group 1  
347 (chryseoviridin). Interestingly, the ATP-grasp ligase of group 5 was indicated to possess  
348 bifunctional activity to catalyse two ester bonds and one isopeptide bond to give the  
349 mature peptide OEP5-1 (Lee et al. 2020b). Recently, an OEP (graspeptide) named  
350 prunipeptin was produced by heterologous expression of the BGC of *Streptomyces*  
351 *prunicolor* (Unno and Kodani 2021). The prunipeptin molecule contained one ester  
352 bond and one isopeptide bond. The ATP-grasp ligase PruB was bifunctional, similar to  
353 the ATP-grasp ligase in group 5. The topology of the intramolecular bridges in  
354 prunipeptin was completely different from that of OEP5-1. As shown in Figure 3A, the

355 precursor peptide MarA is modified by the ATP-grasp enzyme MarB to form one ester  
356 bond and two isopeptide bonds. In the biosynthesis of RiPPs, specific proteases often  
357 cleave the leader peptide region from the precursor peptide. The BGC of  
358 marinomonasin apparently lacks a protease-encoding gene. In the heterologous  
359 expression system, an endogenous protease of *Escherichia coli* seems to cleave the N-  
360 terminus region of the precursor to give mature marinomonasin (Figure 3A). The  
361 bridging pattern of marinomonasin is a new combination of intramolecular bonds (two  
362 isopeptide bonds and one ester bond), and the topology of bridges is novel among  
363 groups of OEPs (graspeptides), as shown in Figure 3B. This indicates that the ATP-  
364 grasp enzyme MarB is a novel bifunctional enzyme that forms two isopeptide bonds and  
365 one ester bond in the molecule. In fact, the amino acid sequence of MarB had low  
366 similarity (less than 35% identity) to other ATP-grasp enzymes of other groups (Table  
367 S4).

368 X-ray crystallography analysis of the ATP-grasp ligase MdnC (group 1) was  
369 accomplished to clarify the reaction mechanism (Li et al. 2016). According to a  
370 previous report (Li et al. 2016), the leader sequence is recognized by the specific  
371 pocket, followed by recruitment of the core peptide region into the active pocket near  
372 the ATP-binding site. In the core peptide, the side chain carboxyl residue of Asp/Glu is

373 phosphorylated using ATP to form the mixed carboxylate-phosphate anhydride, and the  
374 hydroxyl group of Thr or Ser reacts with it to form the ester bond. In the case of other  
375 OEPs (graspeptides), a similar mechanism was proposed (Lee et al. 2020b). The ATP  
376 grasp ligase CdnC was indicated to have dual functions in installing single and bicyclic  
377  $\omega$ -ester rings to afford chryseoviridin (Zhao et al. 2021). X-ray crystallographic analysis  
378 of a quaternary complex including ATP-grasp ligase (CdnC) bound to ADP, the  
379 conserved leader peptide and the peptide substrate illustrated that macrocyclization  
380 occurs in the direction of the *N*- to *C*-terminus of the core peptide. The amino acid  
381 residue Arg 217 in CdnC recognizes the participating Asp residue to lead the substrate  
382 into the active site of the enzyme for phosphorylation (Zhao et al. 2021). In this study,  
383 marinomonasin (OEP/graspeptide in group 7) possessed a novel bridging pattern of  
384 ester and isopeptide bonds, which indicated that the ATP-grasp ligase MarB had a novel  
385 reaction specificity of ligation. The reaction mechanism of MarB is not clear at present,  
386 and further X-ray crystallography experiments are needed to clarify the mechanism.

387

388

### 389 **Author Contributions**

390 I.K. designed and performed experiments. H.N. performed MS and NMR analyses. S.K.

391 conceived and supervised the project. I.K. and S.K. wrote the manuscript.

## 392 **Acknowledgment**

393 We thank Ms. Tomoko Sato for measurement of MS data.

## 394 **Funding information**

395 This study was supported by Grants-in-Aid for Scientific Research: JSPS KAKENHI

396 grant number 20K05848 and 21F21095, Institute for Fermentation, OSAKA (IFO):

397 grant number G-2021-3-010, and Kobayashi Foundation: grant number 196. I. K. was

398 supported by JSPS Postdoctoral Fellowships for Research in Japan (Standard Program).

## 399 **Compliance with ethical standards**

## 400 **Conflict of interest**

401 The authors declare that they have no conflict of interest.

## 402 **Ethical approval**

403 This article does not contain any studies with human participants or animals performed

404 by any of the authors.

## 405 **Data Availability Statement**

406 All data generated or analysed during this study are included in this published article

407 and its supplementary information file.

408

## 409 **References**

410 Ahmed MN, Reyna-Gonzalez E, Schmid B, Wiebach V, Sussmuth RD, Dittmann E,  
411 Fewer DP (2017) Phylogenomic analysis of the microviridin biosynthetic  
412 pathway coupled with targeted chemo-enzymatic synthesis yields potent  
413 protease inhibitors. ACS Chem Biol 12(6):1538–1546.  
414 <https://doi:10.1021/acscchembio.7b00124>

415 Budisa N (2013) Expanded genetic code for the engineering of ribosomally synthesized  
416 and post-translationally modified peptide natural products (RiPPs). Curr Opin  
417 Biotechnol 24(4):591-8. <https://doi:10.1016/j.copbio.2013.02.026>

418 Dehm D, Krumbholz J, Baunach M, Wiebach V, Hinrichs K, Guljamow A, Tabuchi T,  
419 Jenke-Kodama H, Sussmuth RD, Dittmann E (2019) Unlocking the spatial  
420 control of secondary metabolism uncovers hidden natural product diversity in  
421 *Nostoc punctiforme*. ACS Chem Biol 14(6):1271–1279.  
422 <https://doi:10.1021/acscchembio.9b00240>

423 Fujii K, Sivonen K, Naganawa E, Harada K-i (2000) Non-toxic peptides from toxic  
424 cyanobacteria, *Oscillatoria agardhii*. Tetrahedron 56(5):725–733.  
425 [https://doi:10.1016/S0040-4020\(99\)01017-0](https://doi:10.1016/S0040-4020(99)01017-0)

426 Gatte-Picchi D, Weiz A, Ishida K, Hertweck C, Dittmann E (2014) Functional analysis  
427 of environmental DNA-derived microviridins provides new insights into the

428 diversity of the tricyclic peptide family. *Appl Environ Microbiol* 80(4):1380–7.  
429 <https://doi:10.1128/AEM.03502-13>

430 Hemscheidt TK (2012) Microviridin biosynthesis. *Methods Enzymol* 516:25–35.  
431 <https://doi:10.1016/B978-0-12-394291-3.00023-X>

432 Ishitsuka MO, Kusumi T, Kakisawa H, Kaya K, Watanabe MM (1990) Microviridin. A  
433 novel tricyclic depsipeptide from the toxic cyanobacterium *Microcystis viridis*. *J*  
434 *Am Chem Soc* 112(22):8180–8182. <https://doi:10.1021/ja00178a060>

435 Kodani S, Hemmi H, Miyake Y, Kawewan I, Nakagawa H (2018) Heterologous  
436 production of a new lasso peptide brevunsin in *Sphingomonas subterranea*. *J Ind*  
437 *Microbiol Biotechnol* 45(11):983-992. <https://doi:10.1007/s10295-018-2077-6>

438 Lee C, Lee H, Park JU, Kim S (2020a) Introduction of bifunctionality into the  
439 multidomain architecture of the omega-ester-containing peptide plesiocin.  
440 *Biochemistry* 59(3):285-289. <https://doi:10.1021/acs.biochem.9b00803>

441 Lee H, Choi M, Park JU, Roh H, Kim S (2020b) Genome mining reveals high  
442 topological diversity of omega-ester-containing peptides and divergent evolution  
443 of ATP-grasp macrocyclases. *J Am Chem Soc* 142(6):3013–3023.  
444 <https://doi:10.1021/jacs.9b12076>

445 Lee H, Park Y, Kim S (2017) Enzymatic cross-linking of side chains generates a

446 modified peptide with four hairpin-like bicyclic repeats. *Biochemistry*  
447 56(37):4927-4930. <https://doi:10.1021/acs.biochem.7b00808>

448 Li K, Concurso HL, Li G, Ding Y, Bruner SD (2016) Structural basis for precursor  
449 protein-directed ribosomal peptide macrocyclization. *Nat Chem Biol*  
450 12(11):973–979. <https://doi:10.1038/nchembio.2200>

451 Montalban-Lopez M, Scott TA, Ramesh S, Rahman IR, van Heel AJ, Viel JH,  
452 Bandarian V, Dittmann E, Genilloud O, Goto Y, Grande Burgos MJ, Hill C,  
453 Kim S, Koehnke J, Latham JA, Link AJ, Martinez B, Nair SK, Nicolet Y,  
454 Rebuffat S, Sahl HG, Sareen D, Schmidt EW, Schmitt L, Severinov K,  
455 Sussmuth RD, Truman AW, Wang H, Weng JK, van Wezel GP, Zhang Q,  
456 Zhong J, Piel J, Mitchell DA, Kuipers OP, van der Donk WA (2021) New  
457 developments in RiPP discovery, enzymology and engineering. *Nat Prod Rep*  
458 38(1):130-239. <https://doi:10.1039/d0np00027b>

459 Murakami M, Sun Q, Ishida K, Matsuda H, Okino T, Yamaguchi K (1997)  
460 Microviridins, elastase inhibitors from the cyanobacterium *Nostoc minutum*  
461 (NIES-26). *Phytochemistry* 45(6):1197–1202. [https://doi:10.1016/S0031-](https://doi:10.1016/S0031-9422(97)00131-3)  
462 [9422\(97\)00131-3](https://doi:10.1016/S0031-9422(97)00131-3)

463 Okino T, Matsuda H, Murakami M, Yamaguchi K (1995) New microviridins, elastase

464 inhibitors from the blue-green alga *Microcystis aeruginosa*. *Tetrahedron*  
465 51(39):10679–10686. [https://doi:10.1016/0040-4020\(95\)00645-O](https://doi:10.1016/0040-4020(95)00645-O)

466 Philmus B, Christiansen G, Yoshida WY, Hemscheidt TK (2008) Post-translational  
467 modification in microviridin biosynthesis. *Chembiochem* 9(18):3066–3073.  
468 <https://doi:10.1002/cbic.200800560>

469 Reshef V, Carmeli S (2006) New microviridins from a water bloom of the  
470 cyanobacterium *Microcystis aeruginosa*. *Tetrahedron* 62(31):7361–7369.  
471 <https://doi:10.1016/j.tet.2006.05.028>

472 Reyna-Gonzalez E, Schmid B, Petras D, Sussmuth RD, Dittmann E (2016) Leader  
473 peptide-free in vitro reconstitution of microviridin biosynthesis enables design  
474 of synthetic protease-targeted libraries. *Angew Chem Int Ed Engl* 55(32):9398–  
475 9401. <https://doi:10.1002/anie.201604345>

476 Roh H, Han Y, Lee H, Kim S (2019) A topologically distinct modified peptide with  
477 multiple bicyclic core motifs expands the diversity of microviridin-like peptides.  
478 *Chembiochem* 20(8):1051–1059. <https://doi:10.1002/cbic.201800678>

479 Rohrlack T, Christoffersen K, Hansen PE, Zhang W, Czarnecki O, Henning M, Fastner  
480 J, Erhard M, Neilan BA, Kaebernick M (2003) Isolation, characterization, and  
481 quantitative analysis of microviridin J, a new *Microcystis* metabolite toxic to

482            *Daphnia*. J Chem Ecol 29(8):1757–1770. <https://doi:10.1023/a:1024889925732>

483    Shin HJ, Murakami M, Matsuda H, Yamaguchi K (1996) Microviridins D-F, serine  
484            protease inhibitors from the cyanobacterium *Oscillatoria agardhii* (NIES-204).  
485            Tetrahedron 52(24):8159–8168. [https://doi:10.1016/0040-4020\(96\)00377-8](https://doi:10.1016/0040-4020(96)00377-8)

486    Unno K, Kawewan I, Nakagawa H, Kodani S (2020) Heterologous expression of a  
487            cryptic gene cluster from *Grimontia marina* affords a novel tricyclic peptide  
488            grimoviridin. Appl Microbiol Biotechnol 104(12):5293–5302.  
489            <https://doi:10.1007/s00253-020-10605-z>

490    Unno K, Kodani S (2021) Heterologous expression of cryptic biosynthetic gene cluster  
491            from *Streptomyces prunicolor* yields novel bicyclic peptide prunipectin.  
492            Microbiol Res 244:126669. <https://doi:10.1016/j.micres.2020.126669>

493    Weiz AR, Ishida K, Makower K, Ziemert N, Hertweck C, Dittmann E (2011) Leader  
494            peptide and a membrane protein scaffold guide the biosynthesis of the tricyclic  
495            peptide microviridin. Chem Biol 18(11):1413-21.  
496            <https://doi:10.1016/j.chembiol.2011.09.011>

497    Weiz AR, Ishida K, Qwitterer F, Meyer S, Kehr JC, Muller KM, Groll M, Hertweck C,  
498            Dittmann E (2014) Harnessing the evolvability of tricyclic microviridins to  
499            dissect protease-inhibitor interactions. Angew Chem Int Ed Engl 53(14):3735–

500 3738. <https://doi:10.1002/anie.201309721>

501 Zhang Y, Li K, Yang G, McBride JL, Bruner SD, Ding Y (2018) A distributive peptide  
502 cyclase processes multiple microviridin core peptides within a single  
503 polypeptide substrate. *Nat Commun* 9(1):1780. [https://doi:10.1038/s41467-018-](https://doi:10.1038/s41467-018-04154-3)  
504 [04154-3](https://doi:10.1038/s41467-018-04154-3)

505 Zhao G, Kosek D, Liu HB, Ohlemacher SI, Blackburne B, Nikolskaya A, Makarova  
506 KS, Sun J, Barry Iii CE, Koonin EV, Dyda F, Bewley CA (2021) Structural  
507 Basis for a Dual Function ATP Grasp Ligase That Installs Single and Bicyclic  
508 omega-Ester Macrocycles in a New Multicore RiPP Natural Product. *J Am*  
509 *Chem Soc* 143(21):8056-8068. <https://doi:10.1021/jacs.1c02316>

510 Ziemert N, Ishida K, Liaimer A, Hertweck C, Dittmann E (2008) Ribosomal synthesis  
511 of tricyclic depsipeptides in bloom-forming cyanobacteria. *Angew Chem Int Ed*  
512 *Engl* 47(40):7756–7759. <https://doi:10.1002/anie.200802730>

513 Ziemert N, Ishida K, Weiz A, Hertweck C, Dittmann E (2010) Exploiting the natural  
514 diversity of microviridin gene clusters for discovery of novel tricyclic  
515 depsipeptides. *Appl Environ Microbiol* 76(11):3568–3574.  
516 <https://doi:10.1128/AEM.02858-09>

517

518 Figure legends

519 Figure 1. A) biosynthetic gene cluster for marinomonasin (marA and marB) and two  
520 closely located genes including uncharacterized protein coding gene (CUB04734.1) and  
521 quinol monooxygenase coding gene (CUB04736.1), B) alignment of precursor peptides  
522 in group 7 of OEPs (graspeptides), accession numbers are following: <sup>1</sup>CUB04731.1,  
523 <sup>2</sup>WP\_088701948.1, <sup>3</sup>WP\_194089323.1, <sup>4</sup>WP\_039979867.1, <sup>5</sup>WP\_133320119.1,  
524 <sup>6</sup>WP\_033377333.1, <sup>7</sup>WP\_094397536.1, <sup>8</sup>WP\_100996147.1, <sup>9</sup>NOT87337.1,  
525 <sup>10</sup>WP\_128751671.1, <sup>11</sup>WP\_128821517.1, <sup>12</sup>MBB5053603.1, <sup>13</sup>WP\_103684573.1,  
526 <sup>14</sup>WP\_142901796.1, <sup>15</sup>WP\_104805249.1, <sup>16</sup>WP\_008817734.1, <sup>17</sup>WP\_151170560.1,  
527 <sup>18</sup>CRH84860.1, <sup>19</sup>WP\_048393692.1

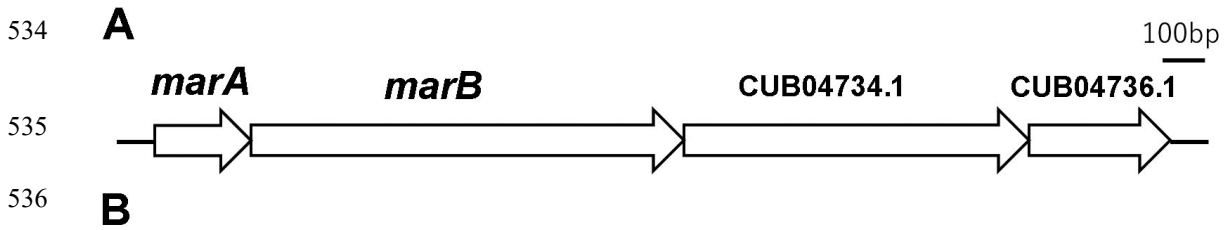
528 Figure 2. Key 2D NMR correlations of marinomonasin

529 Figure 3. A) biosynthetic pathway of marinomonasin, B) topology of intramolecular  
530 bridging patterns in OEPs (graspeptides), ester bond: blue, isopeptide bond: red

531

532

533 Figure 1



<p><i>Marinomonas fungiae</i><sup>1</sup></p> <p><i>Halomonas campaniensis</i><sup>2</sup></p> <p><i>Vibrio hibernica</i><sup>3</sup></p> <p><i>Vibrio sagamiensis</i><sup>4</sup></p> <p><i>Vibrio cholerae</i><sup>5</sup></p> <p><i>Desulfurispora thermophila</i><sup>6</sup></p> <p><i>Thermoanaerobacterium thermosaccharolyticum</i><sup>7</sup></p> <p><i>Lacinutrix</i> sp. Bg11-31<sup>8</sup></p> <p><i>Lysobacter</i> sp.<sup>9</sup></p> <p><i>Tissierellia</i> sp. JN-28<sup>10</sup></p> <p><i>Aeromonas allosaccharophila</i><sup>11</sup></p> <p><i>Afipia massiliensis</i><sup>12</sup></p> <p><i>Marortus luteolus</i><sup>13</sup></p> <p><i>Klebsiella pneumoniae</i><sup>14</sup></p> <p><i>Blautia marasmi</i><sup>15</sup></p> <p><i>Clostridium innocuum</i><sup>16</sup></p> <p><i>Photobacterium damselae</i><sup>17</sup></p> <p><i>Chlamydia trachomatis</i><sup>18</sup></p> <p><i>Pseudomonas lini</i><sup>19</sup></p>	<p>MSNHVLI<del>I</del>ALAKRKPFFVVTPEMPEGCSYDYVRGLW<del>M</del>KANDV-LVSHGSEFGVQATKKCDVETGEDQKGE</p> <p>MSD<del>H</del>VLI<del>T</del>LAKRKPYE<del>V</del>VFNMPPEGCSYDYDRGLW<del>T</del>PKSNEV-LVSHSSEFGVQVTKKCDVETGEDQKGE</p> <p>MSQ<del>H</del>ILIE<del>L</del>AKRKPYSISPEMPENAI<del>F</del>DSAKGY<del>W</del>LSGSEP-LVSPGSKYGALVSKKCDQETGEDQKGE</p> <p>MRQ<del>H</del>ILIT<del>L</del>ATKKPFSEQPEMPEGASYDFSRGY<del>W</del>FKSDE-ILVSYHSEFGT<del>M</del>VSKKCDIETGEDQKGE</p> <p>MQQ<del>H</del>ILIK<del>L</del>ATKKPFSEQPEMPEGTFYDSSRGY<del>W</del>FKSDE-ILVSYHSEFGT<del>M</del>VSKKCDIETGEDQKGE</p> <p>MSN<del>H</del>LLIQ<del>K</del>AYKYPLPKQAPNMDGCYD<del>H</del>KKGY<del>W</del>ISKTNLNPVILDKNFIKPRTKKADRETGEDQKGE</p> <p>MSY<del>H</del>LLIK<del>K</del>AYKYPLPKQV<del>P</del>NMDGCYD<del>H</del>EKGY<del>W</del>ISKTNLNPVILDKNFIKPRTKKEDRETGEDQKGE</p> <p>--MK<del>H</del>ILFQ<del>K</del>ALVYKKRKEITPPKNYEYDYILGAW<del>K</del>DKLSN-LLINSTDFKAQATKKLDIETGEDNKGQ</p> <p>--MH<del>I</del>LEMLAVSSPARDSTPMPIGCQYDFAAGI<del>W</del>K-SEHG-A<del>I</del>LALDPAFEQQT<del>K</del>KMDLETGEDQKQ</p> <p>MLK<del>H</del>LLIE<del>K</del>AYEYPLPHKEPTMQGCKYDNV<del>K</del>GY<del>W</del>TYENNNKPVILDKNFIKPRTKKADRETGEDQKGE</p> <p>MSQ<del>H</del>VLI<del>K</del>LATKKPYLDKPEMPEGSFYDSV<del>K</del>GY<del>W</del>VKAGES-LVSYSSEFGV<del>M</del>ATKKCDIETGEDQKGE</p> <p>MTD<del>H</del>VLIQ<del>L</del>AVRRPHVNAPTLPEGATYDTIS<del>G</del>GW<del>Q</del>TRGE-----GGLTPMSTKKNDIETGEDMKGE</p> <p>MQN<del>H</del>LLIK<del>F</del>AKRKPQKPEMPKGSVFDH<del>K</del>RGI<del>W</del>MYENK-PLVSHTSKFGTQATKKCDVETGEDQKGE</p> <p>MID<del>H</del>ILLQ<del>R</del>SVRRPHSDVPCLGSEVEYRAEEG<del>L</del>WYASSE-----VSKYFRPPMTK<del>F</del>DIETGEDMKGE</p> <p>MKE<del>H</del>ILLD<del>K</del>AYIYENIDRDLSPKDCFYDRM<del>C</del>GL<del>W</del>RVSSTGEVMMVSSVQRAETK<del>K</del>SDIETGEDQKGE</p> <p>MKQ<del>H</del>ILLE<del>K</del>AYCYPEPGEAQIPENCTFIQ<del>K</del>NGY<del>W</del>RNNSTGEIMMLSNDP<del>R</del>RRPQT<del>K</del>KADIETGEDQKGE</p> <p>MQQ<del>H</del>VLI<del>K</del>LATKKPFSEQPEMPEDAFYDNAR<del>G</del>Y<del>W</del>VKAGE-SLVSYNSEYGT<del>M</del>VTKKCDIETGEDQKGE</p> <p>MRE<del>H</del>VLI<del>E</del>KAFMFDNVKEPTKPKGCY<del>D</del>RFVGL<del>W</del>RVDGTGEVMMLSDSFEKPA<del>T</del>KKCDIETGEDQKGE</p> <p>--MH<del>V</del>LQ<del>R</del>KAKTTECSKIDAPEDATYDFEA-<del>G</del>V<del>W</del>RNETG---LVAYDPRHAQST<del>K</del>KNDIETGEDQKQ</p>
--	---

Fig. 1. Kaweewan et al.

537 Figure 2

538

539

540

541

542

543

544

545

546

547

548

549

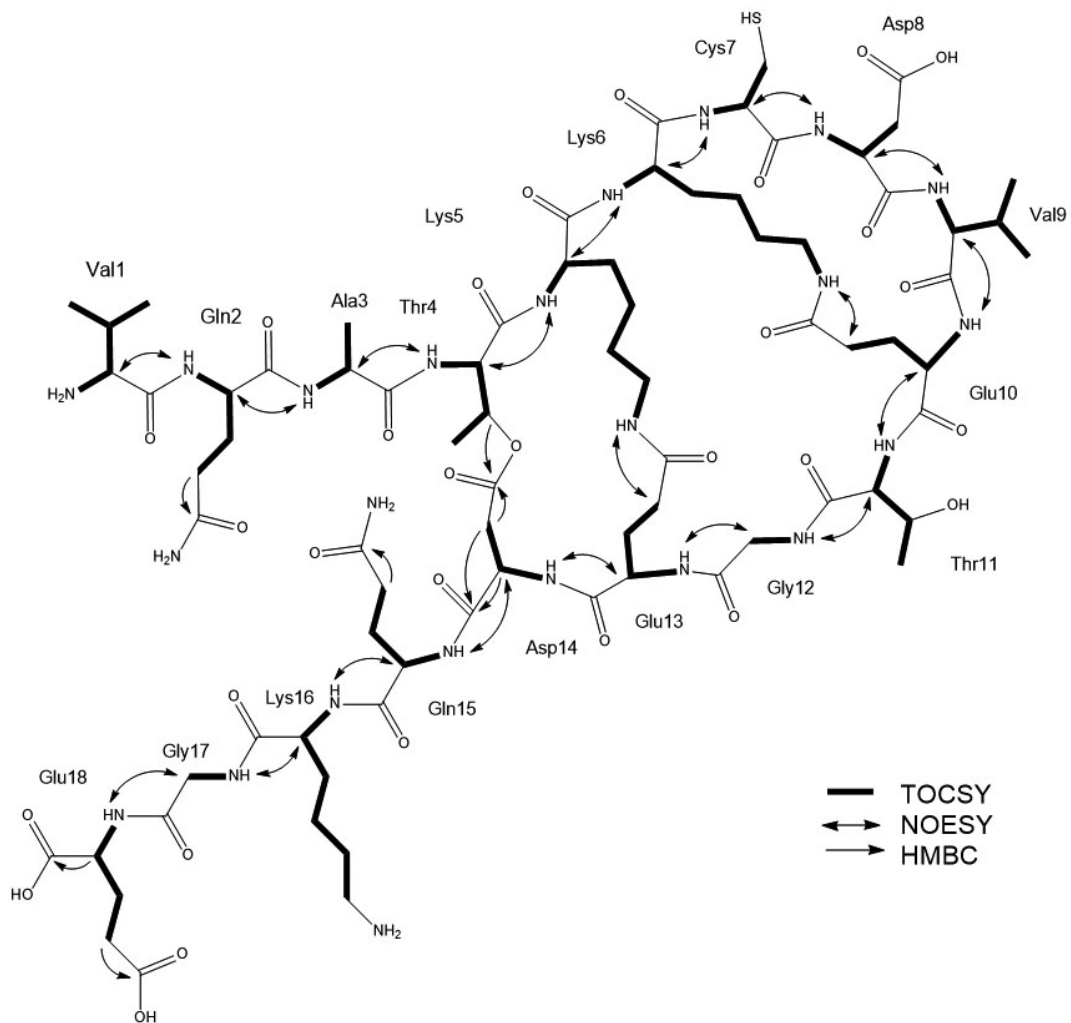


Fig. 2. Kaweewan et al.

550 Figure 3

551

**A**

